Check for updates

Intracerebroventricular Delivery of Human Umbilical Cord Mesenchymal Stem Cells as a Promising Therapy for Repairing the Spinal Cord Injury Induced by Kainic Acid

Fabián Nishida [1,2] · María F. Zappa Villar [2,3,4] · Carolina N. Zanuzzi [1,2,5] · María S. Sisti [1,2] · Agustina E. Camiña [1] · Paula C. Reggiani [2,3,4] · Enrique L. Portiansky [1,2]

Abstract

Spinal cord injury (SCI) is a common pathological condition that leads to permanent or temporal loss of motor and autonomic functions. Kainic acid (KA), an agonist of kainate receptors, a type of ionotropic glutamate receptor, is widely used to induce experimental neurodegeneration models of CNS. Mesenchymal Stem Cells (MSC) therapy applied at the injured nervous tissue have emerged as a promising therapeutic treatment. Here we used a validated SCI experimental model in which an intraparenchymal injection of KA into the C5 segment of rat spinal cord induced an excitotoxic lesion. Three days later, experimental animals were treated with an intracerebroventricular injection of human umbilical cord (hUC) MSC whereas control group only received saline solution. Sensory and motor skills as well as neuronal and glial reaction of both groups were recorded. Differences in motor behavior, neuronal counting and glial responses were observed between hUC-MSC-treated and untreated rats. According to the obtained results, we suggest that hUC-MSC therapy delivered into the fourth ventricle using the intracerebroventricular via can exert a neuroprotective or neurorestorative effect on KA-injected animals.

Keywords Experimental SCI · Fourth ventricle · Stem cell therapy · Neurorestauration · Behavioral tests · Astrocytes · Microglia

Introduction

Spinal cord injury (SCI) is a common pathological condition that leads to permanent or temporal loss of motor and autonomic functions as well as of sensory capacity of tissues and organs innervated by the injured spinal cord segment [1].

Most SCI have two stages of damage: (1) the primary injury, which consists in an acute damage produced by mechanical forces or compression/displacement that can disrupt blood vessels and destroy neurons and glial cells, followed by (2) the secondary injury, that includes a wide range of events, such as oxidative damage by activated radical oxygen,

---

Authors Nishida and Zappa Villar contributed equally to this study.
Senior authors Reggiani and Portiansky contributed equally to this study.

✉ Carolina N. Zanuzzi
carozanuzzi@fcv.unlp.edu.ar

Fabián Nishida
fnishida@fcv.unlp.edu.ar

María F. Zappa Villar
mfzappa@med.unlp.edu.ar

María S. Sisti
mssisti@fcv.unlp.edu.ar

Agustina E. Camiña
aelea@fcv.unlp.edu.ar

Paula C. Reggiani
paulareggiani@conicet.gov.ar

Enrique L. Portiansky
elporti@fcv.unlp.edu.ar

[1] Image Analysis Laboratory, School of Veterinary Sciences, National University of La Plata (UNLP), Calles 60 y 118, 1900, La Plata, Buenos Aires, Argentina

[2] National Research Council of Science and Technology (CONICET), Buenos Aires, Argentina

[3] INIBIOLP, School of Medical Sciences, UNLP, La Plata, Buenos Aires, Argentina

[4] Department of Histology and of Embryology B, School of Medical Sciences, UNLP, La Plata, Buenos Aires, Argentina

[5] Department of Histology and Embryology, School of Veterinary Sciences, UNLP, La Plata, Buenos Aires, Argentina

calcium-mediated damage by calcium ion influx, glutamate excitotoxicity, apoptosis, hemorrhage, inflammation and edema that lead to axonal degeneration, demyelination and cavitation at the site of injury [2, 3]. Therefore, the microenvironment of the spinal cord changes considerably after injury.

There are several ways to experimentally induce SCI. Thus, ischemia and induced traumatisms are two different models of injury of the organ. The mechanisms underlying the pathogenesis of spinal cord ischemia-reperfusion as well as traumatic injury involve intracellular calcium overload, oxygen free radical-mediated lipid peroxidation, inflammation, leukocyte activation, and neuronal apoptosis [4, 5]. The major mediator in the excitotoxic processes is glutamate either released by breakage of the plasma membrane of necrotic neural cells or by massive synaptic release due to unbalance of the membrane potential and increase in intracellular sodium and calcium concentration [5]. However, following trauma to the central nervous system, including SCI, large amounts of ATP and other nucleotides are also released by the damaged tissue. Released ATP acts as an excitotoxin inducing the activation of the purinergic system and leading to a direct calcium-dependent excitotoxic cell death of neurons and oligodendrocytes, or indirectly, favoring glutamate release from neurons and glia [5].

Injection of Kainic acid (KA), an agonist of kainate receptors, a type of ionotropic glutamate receptor, is widely used to induce an in vivo and in vitro experimental neurodegeneration models of CNS [6–10]. In this sense, we have validated the use of KA to induce an in vivo experimental model of neurotoxicity when the drug is injected by intraparenchymal via at the cervical C5 segment of the rat spinal cord [11]. In this model, KA-injected rats showed several motor and sensory impairments of the ipsilateral forelimb correlated with a significant neuronal loss at the corresponding spinal cord segment. We also showed that KA injection alters the intermediate filament expression of neurons at the injection site [12] and induces glial reactivity [13].

The use of Mesenchymal Stem Cells (MSC) therapy applied at the injured nervous tissue has emerged as a promising therapeutic treatment due to their ability to release multiple beneficial factors at the damaged site. Many authors have shown that treatments using MSC were able to reduce inflammatory effects, modulate the response of the immune system, avoid cell apoptosis and reduce scar formation [3, 14–17]. As recently reported by Teng [18], multifunctionality of stem cells allows them to migrate, differentiate and integrate into the tissue allowing them to influence and repair their neighbor cells thus preparing an environment towards the re-establishment of the physiology of organs and system.

Even though some works dealing with the effect of MSC therapy to treat neurodegenerative diseases were published [19–23], in vivo studies for SCI treatment using the intra-cerebroventricular (icv) via are still limited. The goal of the current study was to evaluate the potential therapeutic effect of human umbilical cord (hUC) MSC delivered by icv via on sensory and motor skills of KA-injured animals as well as on their neuron and glial reaction at the injured spinal cord region.

Materials and Methods

hUC-MSC Handling

MSC were isolated from hUC perivascular tissue obtained from healthy donors at the Hospital Universitario Austral (Pilar, Buenos Aires, Argentina) as previously described [24]. Briefly, umbilical cords were dissected and vessels with their surrounding Warthon's Jelly were pulled out. The perivascular Wharton's Jelly was removed from the vessels and mechanically disrupted. Minced fragments were plated in complete DMEM low glucose/20% FBS (Internegocios S.A., Argentina). After 7 days incubation, non-adherent cells and minced fragments were removed and adherent hUC-MSC were cultured and used for different experiments at passages 4 to 6. hUC-MSC were characterized according to the International Society for Cellular Therapy guidelines [25], as previously described [26].

Fluorescent Labeling of hUC-MSC

hUC-MSC cultures were grown in Petri dishes to 90% confluence. Suspended hUC-MSC were labeled with 1,10-dioctadecyl-3,3,30,30-tetramethylindocarbocyanine perchlorate (Dil, Sigma Chem Co.) fluorescent dye (stock solution: $0.25 \ \mu g$ Dil/μl dimethylsulfoxide). Briefly, 10^6 cells/ml trypsinized MSC were suspended in PBS in the presence of Dil (final concentration $1 \ \mu g$/ml) and incubated for 5 min at 37 °C followed by 15 min at 4 °C and finally washed 3 times with PBS. An appropriate dilution (6×10^3 hUC-MSC/μl) for the icv injection was prepared.

Animals and Experimental Design

Young (3 mo. old, 250-350 g) ($n = 12$) male Sprague-Dawley rats, raised in a temperature-controlled room (22 ± 2 °C) on a 12:12 h light/dark cycle were used. Food and water were available ad libitum. All experiments with animals were performed according to the recommendations of the Guide for the Care and Use of Laboratory Animals of the National Institutes of Health. The protocol was also approved by the School of Veterinary Sciences, National University of Plata Institutional Committee for Care and Use of Laboratory Animals (CICUAL), code n° 49-8-15 P.

Rats were randomly divided into three groups, four animals each: **I-Control**, rats that did not receive any treatment; **II-**

KA, each rat was injected with KA and then received saline, and **III-KA + MSC**, each rat was injected with KA solution and then was injected with MSC.

The day of KA injection was defined as the experimental day (ED) **0**. On ED 0 (baseline), 3, 7 and 14, all rats were submitted to a set of motor and sensory tests as described in **2.6**. On ED 3, DiI-labeled hUC-MSC or saline (10 μl) were icv injected into the fourth ventricle (4V) as described in **2.5**. On ED 14, all rats were euthanized as described later (**2.7**) (Fig. 1a).

KA Solution Administration

Before surgery, KA (Sigma-Aldrich, Inc., St. Louis, MO, USA) was dissolved in 0.9% saline and kept at 4 °C until use. On ED 0 and after the behavioral test, rats were anesthetized with ketamine hydrochloride (80 mg/kg; intraperitoneal) plus xylazine (10 mg/kg; intramuscular) and placed in prone position. Animals were injected by intraparenchymal route into the C5 cervical segment with 5 μl of 1 mM KA. The selected concentration induced loss of motor activity of the ipsilateral forelimb as well as loss of neurons, as previously reported [11].

Injections were performed following the protocol described by Nishida et al. [27]. Briefly, trepanation at the C4–C5 fibrous joint 1 mm lateral from the midline (dorsal spinal process) was performed to gain access to the C5 segment. Then, a 10 μl Hamilton® syringe was hand-held and the 26G needle was vertically introduced 1.5 mm down on the right side of the spinal cord to reach the Lamina-VI of that side (ipsilateral). The needle was left in place for 2 min before 5 μl of the KA solution was discharged at a rate of 1 μl/min. Before withdrawal, the needle was held in place for additional 2 min to
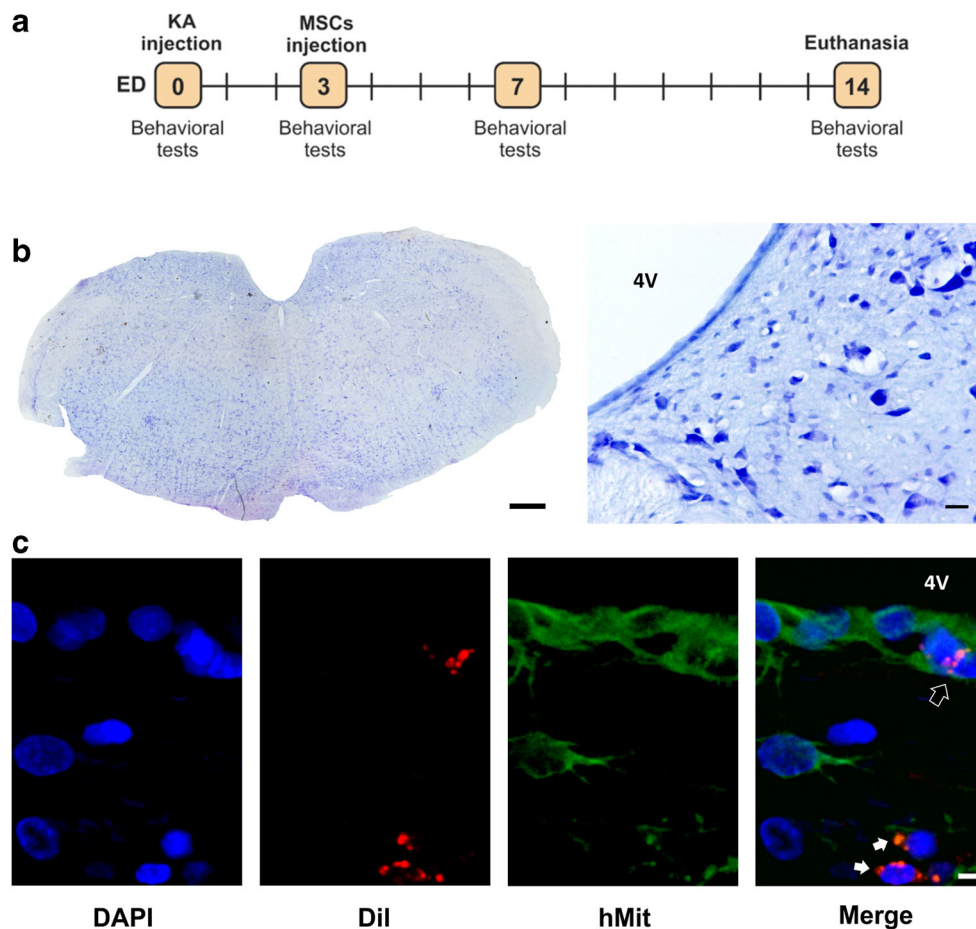

Fig. 1 Experimental design and histological and immunofluorescent aspect of the medulla. Panel **a** illustrates the experimental design of the study. KA and KA + MSC animals were injected with KA on ED 0. MSC were stereotaxically injected into the 4V of KA + MSC rats on experimental day 3. Control group remained intact. On ED 0, 3, 7 and 14 sensory and motor skills were analyzed in all the groups. On ED 14 rats were euthanized by perfusion with a fixative and the spinal cord and brain removed for morphological analysis. Panel **b** shows the cresyl violet staining of the medulla showing an intact parenchyma and 4V ependyma. *Left*: overview. Bar = 0.5 mm; *right*: magnification showing part of the parenchyma of the medulla and the ependyma that covers the 4V. Bar = 20 μm. Panel **c** shows confocal microscopy images of 4V brain sections after DiI-labeled hUC-MSC icv injection. Most of the DiI-labeled hUC-MSC cells remained in contact with the ependymal cell layer (*empty arrow*) while a few of them travelled the medulla parenchyma (*white arrows*). Abbreviation: 4V, fourth ventricle. Bar = 5 μm

avoid leaking of the solution. After surgery animals were kept on a heating pad and checked periodically until they woke up. Thereafter, they were returned to their cages. In no case animals required manual emptying of the bladder.

hUC-MSC Stereotaxic Injection

On ED 3, rats were anesthetized with ketamine hydrochloride (40 mg/kg; intraperitoneal) plus xylazine (8 mg/kg; intramuscular) and placed in a stereotaxic apparatus. To gain access into the 4V, the tip of a 26 G needle fitted to a 50 μl syringe was brought to the following coordinates relative to the bregma: −13.3 mm anteroposterior, −7.5 mm dorsoventral and 0 mm mediolateral [28]. The animals were injected with 10 μl of saline (KA group) of a suspension containing 6×10^4 MSC (KA + MSC group).

Behavioral Tests

Heat Sensitivity Test

The hot-plate test was carried out according to the method previously described [29]. In these experiments, the hot-plate apparatus was set at 55 ± 1 °C. Animals were placed on a 15 cm diameter heated surface surrounded by four acrylic walls, and the time (sec) between placement (time zero) and licking of their forepaws or jumping (whichever occurred first), was recorded and considered as the response latency. A 20 s cut-off was used to prevent tissue damage. Three measurements at 2-min-intervals were taken on each ED.

Suspension from a Horizontal Wire Mesh Pole

The time during which rats could sustain their own weight was determined by placing the animals on a horizontal wire mesh pole. An 8 cm diameter pole was covered by a nylon mesh (pore size: 0.5 cm). The pole was immediately rotated so as the animals were left suspended from the wire mesh 70 cm over a water tank [30]. The latency taken by the animals to fall was recorded as the average of 3 trials with 10 min interval on each ED.

Ladder Rung Walking Test

This test was carried out to examine forelimb coordination during skilled walking in rats according to Metz and Whishaw [31]. Rats were trained to walk across the ladder rung walking apparatus 1 week before the experiment. The rung pattern (1–3 cm apart between rungs) was not altered during all ED. For the evaluation, three trials were video recorded per session per animal and presented as an average performance per group. Limb coordination and skilled walking patterns were analyzed according to a scoring system published by Metz and Whishaw [31] ranging from 0 (abnormal) to 6 (perfect). For this work, the total score per group and experimental day for ipsilateral and contralateral forelimb were considered. The video recording was taken from a lateral view with a digital video camera (Panasonic DMC-FH1, China), and the shutter speed was set at 30 f/s. The recordings were analyzed frame-by-frame to classify all the steps per group.

Spinal Cord Collection and Processing

Immediately before euthanasia rats were placed under general anesthesia by injection of ketamine hydrochloride (80 mg/kg, i.p.) plus xylazine (10 mg/kg; i.m.) and then intracardiacally perfused with a 4% buffered saline-paraformaldehyde solution. The skull and the vertebral column were removed and post-fixed in 10% buffered formaldehyde for 24 h. Brain and spinal cord were then dissected, immersed in cryopreservation buffer (30% sucrose, 1% polyvinylpyrrolidone, 30% ethylene glycol, 1% 1 M phosphate buffer and distilled water to 100 ml) and stored at −20 °C until use.

Medulla and the C5 segment were cut into 0.5 cm thick coronal sections under a magnifying glass and then placed at the center of a well in a 48-well plate. The well was then filled with 0.5 ml jellifying solution (10% sucrose in 1 M phosphate buffer and 4% low melting point agarose [Sigma Chemical Co., St. Louis, MO]) and stored at 4 °C until a jelly block was formed. Then, blocks of tissue were serially cut into 20 μm thick coronal sections using a vibratome (Leica VT 1000S, Germany). From each block, three to five sections, 120 μm apart, were mounted on jellified slides (6 g unflavored gelatin, 0.5 g $KCr(SO_4)_2.12 H_2O$ and distilled water to 300 ml), and stained with the cresyl violet technique for histopathological analysis.

Immunohistochemistry (IHC) and Immunofluorescence (IF) Techniques

Immunohistochemistry technique was used to evaluate changes in neurons, astrocytes and microglia cell population. For these purposes spinal cord sections were immersed in PBS with 0.03% H_2O_2 for 30 min at room temperature to block endogenous peroxidase. Sections were then rinsed twice in PBS. Then, sections were exposed to microwave antigen retrieval using a citrate buffer solution, pH 6.0 and then washed twice with PBS. Later, all sections were incubated with 1% bovine serum albumin (BSA) for 30 min, followed by overnight incubation either with the anti-NeuN (Neuronal Nuclear Antigen) monoclonal antibody (Clone A60 Biotinylated, lot LV1770323, Millipore, CA, USA; diluted 1:200) for identifying neurons, anti-GFAP (Glial Fibrillary Acidic Protein) polyclonal antibody (Ref Code IR524, DakoCytomation, Carpinteria, CA, USA; ready to use) to identify intermediate

filaments in astrocytes or anti-IBA-1 (Ionized Calcium-Binding Adapter molecule 1, encoded by the AIF-1 gene) polyclonal antibody (AIF-1, lot A106554, Sigma-Aldrich, St Louis, MO, USA; diluted 1:500) to label microglial cells. Sections were then rinsed with PBS and incubated with the EnVision© detection system + HRP system labeled anti-mouse or anti-rabbit polymer (DakoCytomation, Carpinteria, CA, USA) for 45 min. Finally, sections were rinsed in PBS and the reaction was revealed with the liquid chromogen 3,3-diaminobenzidine tetrahydrochloride (Vector Laboratories Inc., CA, USA). Hill's hematoxylin was used for counterstaining. Control negative sections were prepared by omitting primary antibody.

To confirm the presence of Dil-labeled hUC-MSC at the injection site the immunofluorescence technique was applied on medulla sections including the fourth ventricle (4V) ependyma. Sections were rehydrated with PBS containing 0.05% Tween-20 for 10 min at room temperature and then exposed to microwave antigen retrieval using a buffer citrate solution, pH 6.0. Then, sections were incubated with 1% BSA in PBS for 30 min, followed by overnight incubation with anti-human mitochondrial marker (hMit, Cat# MBS438169, monoclonal, MyBioSource, San Diego, California, USA; diluted 1:400). Sections were then rinsed threefold in PBS and incubated with 1:1000 Alexa Fluor 488-conjugated anti-mouse (Invitrogen, Thermo Fisher Scientific Inc.) secondary antibody for 45 min. Then, sections were rinsed threefold in PBS and counterstained for 15 min with the fluorescent DNA stain 4,6-diamidino-2-phenylindole (DAPI). Control negative sections were prepared by omitting primary antibody.

Image Analysis

Images of IHC stained spinal cord sections were captured using a digital RGB video camera (Olympus DP73, Japan) attached to a microscope (Olympus BX53, Japan). To create a map of the entire segment stitched images using a 20x objective were captured using the Multiple Image Alignment (MIA) function of a digital image analyzer (cellSens Dimension, V1.7, Olympus Corporation, Japan). No further processing was necessary after obtaining the original images. To determine the total number of positively labeled cell bodies or positively stained area per section, color segmentation was performed [32]. All observations were done by two independent, double-blind researches to obtain a more objective counting.

Images of IF sections were captured using a confocal microscope (FV100, Olympus). Neuronal cell counting was carried out on anti-NeuN as well as on cresyl violet stained samples. Glial cell counting was carried out on anti-GFAP (astrocytes) and anti-IBA-1 (microglia) immunohistochemically stained images. Determination of immunohistochemically stained area was also considered for anti-GFAP and anti-IBA-1. For each spinal cord section, the ipsilateral and contralateral sides of the C5 segment were considered as separated.

For determination of the number of neurons, three areas of analysis were considered: dorsal grey matter (Paxinos Laminae I-V), medial grey matter (Paxinos Laminae VI and X), and ventral grey matter (Paxinos Laminae VII-IX) [11]. All measurements were performed using the ImagePro Plus image analysis software (v6.3, Media Cybernetics, MA, USA).

Statistical Analysis

Statistical analyses were performed using the GraphPad Prism 6 software (Graph-Pad Software, San Diego, CA, USA). Data corresponding to behavioral tests were analyzed by two-way analysis of variance (ANOVA) with repeated measures to compare the motor and sensory performance at different tests between groups at different time points. Cell counting, and area were compared by One-way ANOVA and for multiple comparisons, Tukey Kramer Multiple-Comparison Test was used as a post-hoc test. Significance was assumed at values of $P < 0.05$.

Results

hUC-MSC in the 4V

Cresyl violet staining of medulla showed no lesions neither at parenchyma nor at the 4V ependyma where hUC-MSC were delivered (Fig. 1b). Dil-labeled hUC-MSC were positive to anti-human mitochondria antibody (Fig. 1c). They were found at the 4V ependymal layer of KA + MSC animals. Some of these cells were also found closer to the ependyma, inside the medulla gray matter.

hUC-MSC Therapy Improves the KA-Affected Motor Performance

The latency time in the heat sensitivity test showed no significant differences among groups at any time point (Fig. 2a. **Two-way ANOVA with RM, $F_{(2, 9)} = 1.412$, $P = 0.2929$**). In contrast, tasks requiring more coordinated control of motor and reflexive responses such as suspension from a horizontal wire mesh pole showed significant declines with KA on ED 7 and 14. No significant differences were found between KA + MSC and Control animals at any time point (Fig. 2b. **Two-way ANOVA with RM, $F_{(2, 9)} = 9.312$, $P = 0.0064$**). In addition, in the ladder rung walking test, the total score of the ipsilateral forelimb revealed that KA animals showed a significant impairment in their motor performance from ED 3 up to ED 14, whereas KA + MSC group showed a not significant impairment in their performance at ED 3 and then a gradual

Fig. 2 **Behavioral tests**. All these tests were performed to determine the sensory and motor skill of MSC treated and untreated animals. Estimated mean responses for: heat sensitivity test **a**; suspension from a horizontal wire mesh pole **b**; and ladder rung walking test at the ipsilateral **c** and contralateral **d** forelimb sides. In all cases data are expressed as estimated mean ± SEM. Comparisons were made between groups. Control vs. KA group: $*P < 0.05$; $**P < 0.01$; $***P < 0.001$. KA vs. KA + MSC group: $^+P < 0.05$; $^{+++}P < 0.001$. Undepicted comparisons account for a not significant difference between groups
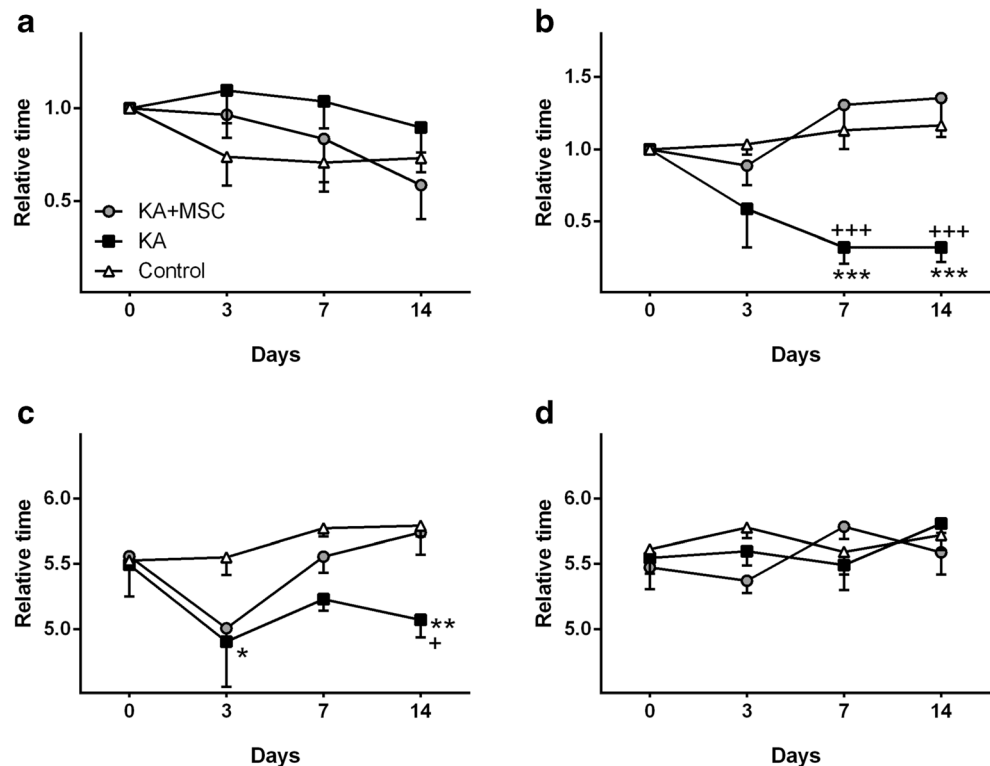
improvement from this day to the end of the experiment at ED 14 (Fig. 2c. *Two-way ANOVA with RM, $F_{(2, 9)} = 8.567$, $P = 0.0083$*). Control animals showed no alteration in their performance along experimental days. Statistical analysis showed a significant difference in the total score of KA animals vs. KA + MSC and Control animals at ED 7 and 14. No significant differences were observed between KA + MSC and Control rats at any time point. No alterations were observed in the total score of the contralateral forelimb of all groups with no significant differences among groups at any time point (Fig. 2d. *Two-way ANOVA with RM, $F_{(2, 9)} = 0.8113$, $P = 0.4743$*).

hUC-MSC Therapy Protects Neurons of the Spinal Cord in the KA-Neurotoxicity Model

Figure 3a, b shows the histological aspect of KA and KA + MSC C5 spinal cord segments at ED 14. Histological aspect of neurons was similar in all the groups. Comparison of dorsal, medial and ventral areas of the spinal cord sections showed a significant reduction in the neuronal counting of KA rats only at the ipsilateral ventral and medial areas as compared to Control rats (Fig. 3c. *One-way ANOVA, $F_{(2, 9)} = 10.52$, $P = 0.0044$*); interestingly, KA + MSC sections showed a significant increase in the neuronal counting at the ipsilateral ventral area as compared to KA sections (Fig. 3d. *One-way ANOVA, Ventral: $F_{(2, 9)} =*

12.48, $P = 0.0025$. Medial: $F_{(2, 9)} = 4.837$, $P = 0.0375$. Dorsal: $F_{(2, 9)} = 2.499$, $P = 0.1370$*).

Counting of neurons at the contralateral C5 section showed a significant reduction in the KA animals as compared to the Control group (Fig. 3e. *One-way ANOVA, Total: $F_{(2, 9)} = 4.923$, $P = 0.0359$*). When dorsal, medial and ventral areas of the section were separately considered the analysis revealed that KA induced a significant reduction in the neuronal counting only at the contralateral ventral area (Fig. 3f. *One-way ANOVA, Ventral: $F_{(2, 9)} = 5.427$, $P = 0.0284$*). No reduction in number of neuronal cells at the contralateral dorsal and medial areas of any group were observed (Fig. 3f. *One-way ANOVA, Dorsal: $F_{(2, 9)} = 1.481$, $P = 0.2779$. Medial: $F_{(2, 9)} = 2.054$, $P = 0.1842$*).

Effects of hUC-MSC Therapy on Microglia

KA injection at the spinal cord produced an overwhelming inflammatory microgliosis (Fig. 4a, b). To evaluate a possible immunomodulatory effect of hUC-MSC in the spinal cord after KA-induced damage, the microglia reaction was analyzed.

Immunohistochemistry with anti-IBA-1 antibody revealed a significant increase in the number of positive cells in the KA group in comparison to Control animals for both, ipsilateral and contralateral sides. On the contrary, hUC-MSC treatment in the KA + MSC rats induced a significant decrease in the number positive cells at the ipsilateral side as compared to KA
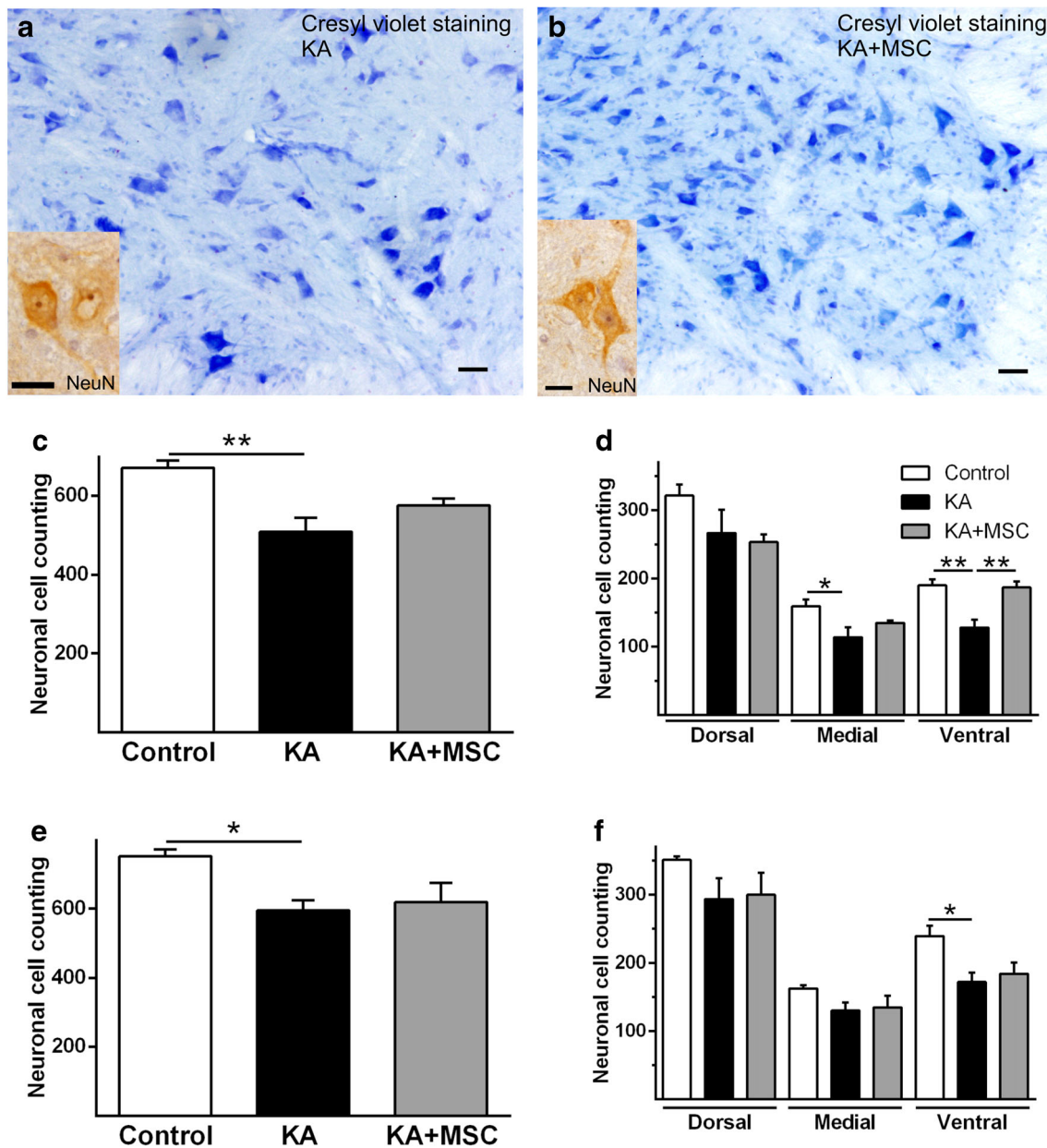
Fig. 3 Counting assessment of neuronal population at the C5 segment. For counting neurons, either cresyl violet stained or NeuN positive cells were used. Panel **a** shows cresyl violet KA injected C5 segment medial and ventral area at ED 14. Panel **b** shows the same segment of KA + MSC animals. Bar = 20 μm. Insets show NeuN stained cells. Although in smaller amount, no structural differences were observed in the positive cells of both groups. Bar = 20 μm. NeuN positive cells showed a significant reduction in the neuronal counting of KA group sections as compared to the Control group, both at the ipsilateral and contralateral forelimb sides of the C5 segment (**c** and **d**, respectively). Analysis of dorsal, medial and ventral section areas revealed a significant reduction in the neuronal counting at the ipsilateral ventral and medial areas (**e**) and at the contralateral ventral area (**f**) of KA group as compared to Control. In all cases, data are expressed as estimated mean ± SEM. Comparisons were made between groups. *$P < 0.05$; **$P < 0.01$. Undepicted comparisons account for a not significant difference between groups

animals; however, it did not reach the values of the Control group. No significant differences were found between KA + MSC and Control animals at the contralateral side (Fig. 4c. *One-way ANOVA, Ipsilateral: $F_{(2, 9)} = 58.04$, $P < 0.0001$; 4E. One-way ANOVA, Contralateral $F_{(2, 9)} = 6.507$, $P = 0.0179$*). Besides, the IBA-1 immunostained areas of KA animals were significantly larger than those found in KA + MSC and Control animals for both, ipsilateral and contralateral sides. The hUC-MSC treatment induced a significant decrease in the IBA-1 immunostained areas as compared to KA counterparts while no significant differences were found between KA + MSC and Control animals at both sides (Fig. 4d.
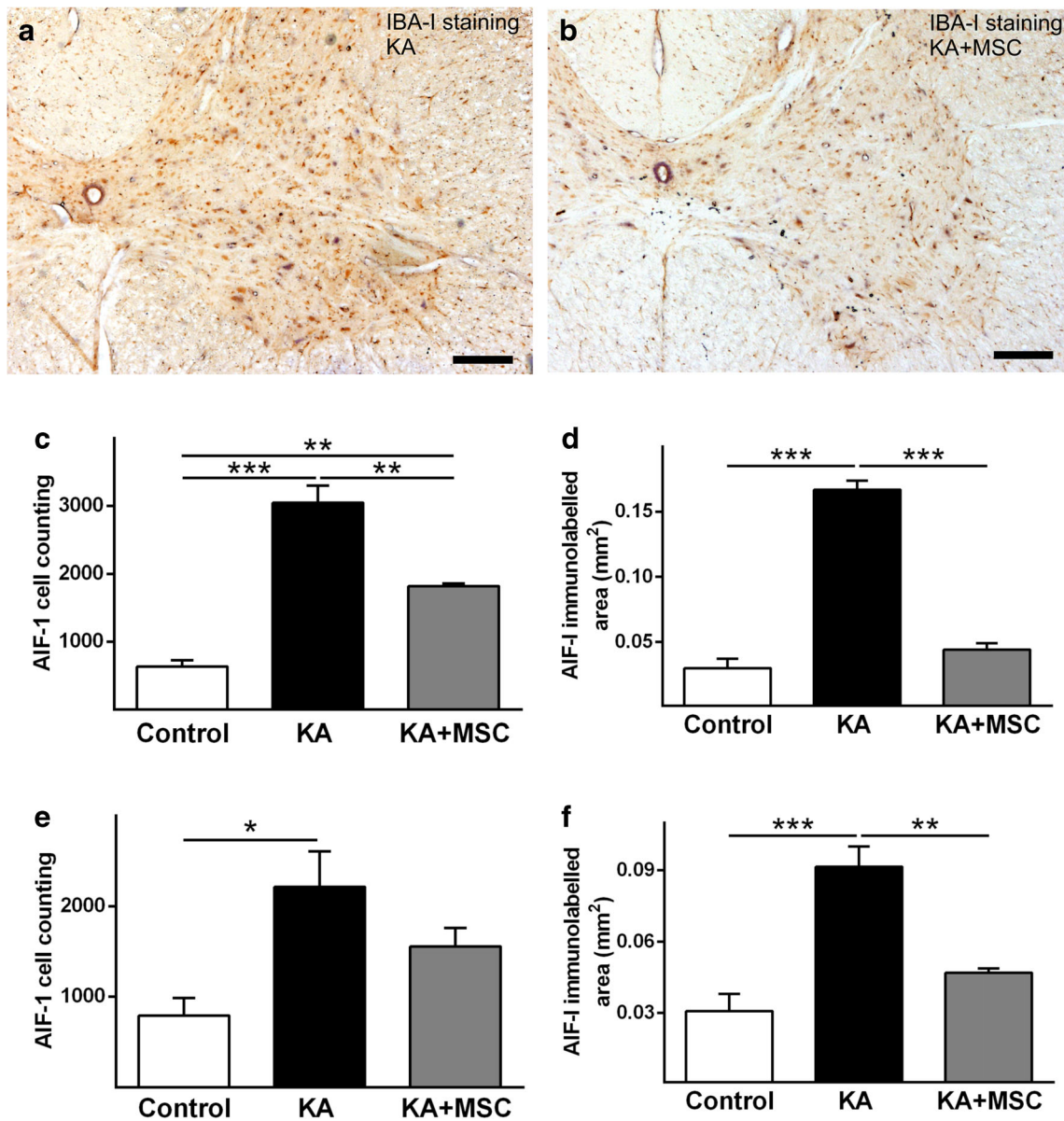
Fig. 4 IBA-1 immunoreactive cells counting. IBA-1 immunoreactive cells at the forelimb ipsilateral side of the C5 segment in KA animals **a** and KA-MSC rats **b**. Bar = 200 μm. IBA-1 positive cells showed a significant increase in KA group sections as compared to Controls at the ipsilateral **c** and **d** and contralateral **e** and **f** forelimb sides of C5 segment. MSC-treatment revealed a significant reduction in the IBA-1 counting at the ipsilateral side **c** and in the IBA-1 immunoreactive area at both ipsilateral and contralateral forelimb sides (**d** and **f**, respectively) as compared to KA group. In all cases, data are expressed as estimated mean ± SEM. Comparisons were done between groups. *$P < 0.05$; **$P < 0.01$; ***$P < 0.001$. Undepicted comparisons account for a not significant difference between groups

One-way ANOVA, Ipsilateral: $F_{(2, 9)} = 131.2, P < 0.0001$; 4F. One-way ANOVA, Contralateral: $F_{(2, 9)} = 23.07, P = 0.0003$).

Effects of hUC-MSC Therapy on Astroglial Cells

Astrocytes were identified by GFAP immunostaining in the spinal cord C5 segment (Fig. 5a–c). Total number of astroglial cells of both, ipsilateral and contralateral sides were significantly increased in KA and KA + MSC animals in comparison to Control animals. No significant differences were found between KA + MSC and KA animals at both sides (Fig. 5d. *One-way ANOVA, Ipsilateral: $F_{(2, 9)} = 21.56, P = 0.0004$; 5F. One-way ANOVA, Contralateral $F_{(2, 9)} = 32.02, P < 0.0001$).* The GFAP immunostained areas of KA + MSC animals were significantly larger than those found in Control animals for both, ipsilateral and contralateral sides (Fig. 5e. *One-way ANOVA, Ipsilateral: $F_{(2, 9)} = 6.533, P = 0.0177$; 5G. One-way ANOVA, Contralateral $F_{(2, 9)} = 5.359, P = 0.0293$).*
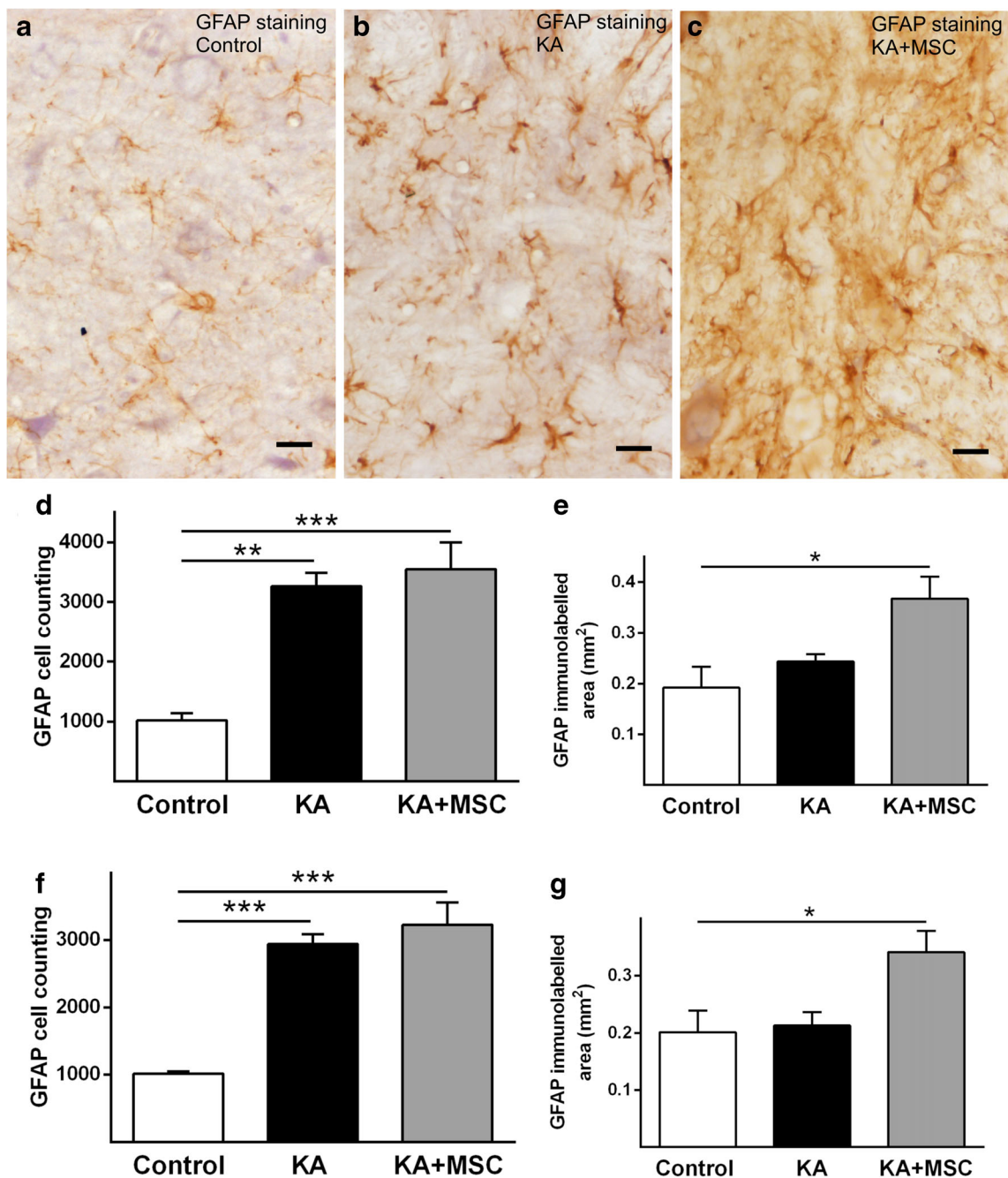
Fig. 5 GFAP immunoreactive cells counting. GFAP immunoreactive cells at the forelimb ipsilateral side of the C5 segment in control **a**, KA animals **b** and KA-MSC rats **c**. Significant differences were found between KA-injected and Control group in GFAP cell counting **d** and **f**. hUC-MSC treatment revealed a significant increase in the GFAP cell counting and GFAP immunoreactive area (**d**, **e** and **f**, **g**) as compared to Control group. In all cases, data are expressed as estimated mean ± SEM. Comparisons were made between groups. *P < 0.05; **P < 0.01; ***P < 0.001. Undepicted comparisons account for a not significant difference between groups

Discussion

Local and systemic delivery are two principal methods to introduce MSC. Both show advantages and disadvantages. Thus, the optimal delivery method will depend on which mechanisms of action of the MSC need to be promoted.

However, it is known that the therapeutic efficacy of delivered MSC will increase dramatically if they are efficiently directed to the injury site [33].

Some years ago, a physical continuity between the rat 4V and the spinal cord central canal was demonstrated [30]. This communication path is of particular interest for setting up

protocols for treating spinal cord injuries thus avoiding the loss of cellular or chemical reagents in the extraneural compartments. Therefore, we propose the use of the icv route for hUC-MSC therapy in SCI. The safety, feasibility and therapeutic efficacy of this route was shown in a mouse intracerebral hemorrhage model using bone marrow stem cells [34] and for intracerebral tumor treatment using neural stem cells [35].

Using the icv route, 11 days after their injection surviving Dil-labeled hUC-MSC were observed in the 4V ependymal layer and in the parenchyma of the medulla. Arguments for local injection include not only the delivery of MSC near to the site of the injury, but also the possibility of MSC to migrate towards the injured tissue [33]. In the present study we could not detect Dil-labeled hUC-MSC in the cervical spinal cord parenchyma of treated rats although this region is close to their delivery site. A similar result was reported by Huang et al. [34], when using icv delivery of bone marrow stem cells for intracerebral hemorrhage treatment. It was suggested that locally injected cells can be lost by wash out, cell death or rejection by the immune system when they begin their differentiation. Nevertheless, the improvement in the motor behavior, neuronal cellular counting and glial reaction found in the KA injured-animals may be attributed to the autocrine and paracrine activity of hUC-MSC, by local releasing of cytokines and growth factors or by further differentiating into other cells [17, 33].

The use of hUC-MSC in preclinical studies have shown that these cells have a promising profile of neurotrophic, anti-apoptotic, and anti-inflammatory effects [36, 37]. Moreover, the risk of graft rejection using hUC-MSC is very low as confirmed by studies demonstrating their hypoimmunogenicity [38].

Here, we found differential effect on glial cells and neurons. Little is known regarding the mechanism underlying the interactions between hUC-MSC and neurons and glial cells. During SCI glial cells show responses that shift over time and may produce both beneficial and detrimental effects on the tissue [39, 40]. The detrimental functions of reactive astrocytes are in fact responses to injury with the aim of protecting the nervous system and less affected tissue by healing the damaged area and limiting further extension of the injury. Nevertheless, astrogliosis can also be beneficious to the repairing process by secreting growth-promoting neurotrophic factors and thus contributing with the endogenous neuroprotection [40].

Astrogliosis after SCI shows variable intensity which depends on the initial severity of the lesion and the length of post-injury time. During the first 2 weeks after SCI the astrocytic scar is consolidated in order to create a physical barrier and promote tissue restauration [39]. Scar forming astrocytes can help restrict the spread of toxic aspects of inflammation, thereby preventing lesion expansion and further loss of function. However, reactive astrocytes in the glial scar secrete different molecules that may prevent axon plasticity and limit post-SCI repair [39]. In our study, although hUC-MSC did not reduce the astrocytic reaction as was observed in other studies [1, 41, 42], no detrimental effects on functional recovery, as shown by the improved motor performance in KA + MSC group in comparison to the KA-group were observed. As was mentioned by Lukovic et al. [40] stem cell therapy should produce an adequate microenvironment in order to provide the proper astrocytic response in spatial and time length.

Regarding microglial cells, here we showed a significant reduction of these reactive cells in KA + MSC group as compared to KA group. According to Gaudet and Fonken [39] microglia showed a balance between pro- and anti-inflammatory phenotypes by day 7 post-SCI. From this time point on the response turns predominantly pro-inflammatory. In our model, we showed that hUC-MSC therapy contributed to the reduction of microglia response, apparently ameliorating the deleterious proinflammatory response of these cells.

By using conditioned media from hUC-MSC Salgado et al. [43] showed that these cells can potentiate astrocyte and oligodendrocyte cell densities, without stimulating the proliferation of microglial cells, and suggested that hUC-MSC release factors to the extracellular milieu that have different direct impact on the densities of each type of glial cells, possibly due to the existence of variable sensitivity. Different therapeutic methods have been studied to minimize the damage in central nervous system injuries. These methods aimed to promote neuronal circuits reconnection or neuronal re-growth at the injured site. As mentioned by Abbaszadeh et al. [44], mature neurons could re-extend their axon partly depending on the availability of neurotrophic factors at the required site. Also, the availability of these factors may be improved by modulating their gene expression.

It has been shown that injection of stem cells into the injured CNS exert a neuroprotective effect. Hofstetter et al. [45] and Ohta et al. [46] showed that bone marrow stromal cells administered into the injured spinal cord of rats promoted a protective effect against cell death. It was suggested that MSC are capable of combine trophic support, anti-inflammatory effect, immunomodulation, anti-apoptotic effect, neutralization of inhibitory factors and reduction of scar formation by secreting several growth factor molecules in the injured CNS, thus contributing with the restoration of the functioning of the damaged tissue [3]. Moreover, some authors suggest that stem cells are also capable of being integrated into the CNS and to reestablish the damaged circuit [47, 48], as well as restoring motor and sensory tasks in SCI models [49, 50].

According to our results, at the end of the experiment the number of NeuN positive cells in hUC-MSC-injected animals did not differ from that of Control animals, while KA-injected animals showed a significant reduction in NeuN positive cells mainly at the ventral region of the spinal cord segment. In

other studies, using the intravenous administration of hUC-MSC 24 h after cerebral ischemia, a significant recovery in neurological injury was reported with a reduction of hypertrophic microglia and an increase in neuron and neuroblast migration in the ipsilateral brain regions [51]. As analyzed by Cofano et al. [17], stem cell therapy in SCI injury remains an experimental therapy and may be used in association with others.

Recently, we have shown that glial cells undergo morphometric changes as well as increase in their number due to the excitotoxic effects of KA [13]. Interestingly, here we have shown that microgliosis decreased after hUC-MSC therapy. In concordance, the intrathecal injection of hUC-MSC also suppressed the activation of microglia and astrocytes in a model of neuropathic pain by reducing the production of pro-inflammatory cytokines and up regulating anti-inflammatory cytokines [42].

Taken together the effect on neurons and microglial cells, it is possible to speculate that hUC-MSC engraftment restored neuronal population and modulated the microglia, instances that could be enough to restore the motor function in the SCI model. This restorative effect could be mediated by the known regenerative [51, 52] and immunoregulatory properties of MSC [53, 54]. In agreement, it was reported that bone marrow-derived MSC were able to control microglial activation through the production of several factors, which suggests that MSC could be a promising therapeutic tool for the treatment of microgliosis-associated diseases [55].

Astrogliosis is a complex multifactorial process that can occur after SCI. In fact, during traumatic SCI astrogliosis, reactive astrocytes that have neuroprotective properties, coexist with scar-forming astrocytes that inhibit axonal regeneration as well as functional recovery [56]. Although it is widely recognized that MSC and MSC-based treatment are emerging as a promising therapy for SCI, it is still controversial to decide an optimal timing of treatment. It was observed that astrogliosis increased with MSC transplantation 7 days after SCI. The lesion core area and the number of astrocytes increased in MSC-treated group as compared to SCI group [57].

Recently, reactive astrocytes were further classified according to their functions into harmful A1 and neuroprotective A2 astrocytes [58, 59]. These findings can well explain the dual effects of reactive astrocytes in central nervous injuries and diseases. Interestingly, it has been shown that icv MSC-derived therapy promoted functional behavioral recovery and reduced lesion tissue area 28 days after traumatic SCI in rats by the suppression of the A1 reactive astrocytes [60]. In this line, intravenously injected MSC and MSC-exosomes reduce SCI-induced A1 astrocytes, probably via inhibiting nuclear translocation of NFκB p65, and exert anti-inflammatory and neuroprotective effects following SCI [56]. In a different neurodegenerative rat model, we observed that GFAP area could not be reversed by the long-term hUC-MSC therapy [61]. In accordance with this previous work,

our results showed that hUC-MSC-injected animals increased the GFAP cell number and GFAP positive area in comparison to Control animals at the forelimb ipsilateral side, 11 days after MSC injection. Thus, we suggest that different subtypes of reactive astrocytes might play dual roles in SCI. Consequently, further studies are needed to elucidate both, whether reactive astrocytes have a bilateral role in SCI and the effect of MSC on astroglia in our excitotoxic SCI rat model.

On the other side, it has been proposed that astrocytes control the neurogenic niches of neural stem cells to regulate their function [62]. Moreover, activated astrocytes promote brain-derived neurotrophic factor secretion which may benefit to both neural differentiation of exogenic hUC-MSC and endogenic neurogenesis [63]. Taken together we can speculate that the increase in GFAP area in KA-MSC animals represents a massive activation of astrocytes that would contribute to foreign and local stem cell stimulation and differentiation into mature neurons to repopulate the damaged tissue.

How stems cells contribute with the repairing of SCI is still under revision. It was proposed that MSC secrete exosomes which can modulate a hostile environment through a paracrine action [64]. It was observed that systemic administration of MSC exosomes significantly attenuated the lesion size and improved functional recovery after SCI. Moreover, it attenuated cellular damage in the injured spinal cord. Since the same outcome was observed in our KA-MSC animals, we can speculate that exosomes released by hUC-MSC are contributing with the functional and tissue recovery of MSC-treated animals.

In this work, we described the 2 weeks therapeutic effects of hUC-MSC injected into the 4V on the excitotoxic effect induced by the intraparenchymal injection of KA. Wrathall et al. [65] initially showed that SCI repair mechanisms are different in the short and long term. In their model, the authors used KA antagonists to reverse the lesions induced by it. In our model, we use hUC-MSC with the intention of generating different mediators that could counteract not only the effects of KA but also reverse the damage induced by other spinal injury mechanisms.

Since no cytokine nor cell integration analysis were carried out further studies are needed to elucidate the mechanism involved in the improvement observed in hUC-MSC-treated animals and to associate clinical with morphological changes observed. Nevertheless, we can conclude that icv therapy using hUC-MSC delivered into the 4V can exert a neuroprotective or neurorestorative effect on KA-injected animals.

Compliance with Ethical Standards

Conflict of Interest   The authors do not have any financial conflict of interests to disclose.

Research Involving Animals   All experiments with animals were performed according to the recommendations of the Guide for the Care and Use of Laboratory Animals of the National Institutes of Health. The protocol was also approved by the School of Veterinary Sciences, National University of Plata Institutional Committee for Care and Use of Laboratory Animals (CICUAL), code n° 49-8-15 P.

References

1. Nicola, F., Marques, M. R., Odorcyk, F., Petenuzzo, L., Aristimunha, D., Vizuete, A., Sanches, E. F., Pereira, D. P., Maurmann, N., Gonçalves, C. A., Pranke, P., & Netto, C. A. (2019). Stem cells from human exfoliated deciduous teeth modulate early astrocyte response after spinal cord contusion. *Molecular Neurobiology, 56*(1), 748–760. https://doi.org/10.1007/s12035-018-1127-4.

2. Nejati-Koshki, K., Mortazavi, Y., Pilehvar-Soltanahmadi, Y., Sheoran, S., & Zarghami, N. (2017). An update on application of nanotechnology and stem cells in spinal cord injury regeneration. *Biomedicine Pharmacotherapy, 90*, 85–92. https://doi.org/10.1016/j.biopha.2017.03.035.

3. Papa, S., Vismara, I., Mariani, A., Barilani, M., Rimondo, S., De Paola, M., Panini, N., Erba, E., Mauri, E., Rossi, F., Forloni, G., Lazzari, L., & Veglianese, P. (2018). Mesenchymal stem cells encapsulated into biomimetic hydrogel scaffold gradually release CCL2 chemokine in situ preserving cytoarchitecture and promoting functional recovery in spinal cord injury. *Journal of Controlled Release, 278*, 49–56. https://doi.org/10.1016/j.jconrel.2018.03.034.

4. Chen, S., Yi, M., Zhou, G., Pu, Y., Hu, Y., Han, M., & Jin, H. (2019). Abdominal aortic transplantation of bone marrow mesenchymal stem cells regulates the expression of ciliary neurotrophic factor and inflammatory cytokines in a rat model of spinal cord ischemia-reperfusion injury. *Medical Science Monitor, 25*, 1960–1969. https://doi.org/10.12659/MSM.912697.

5. Reigada, D., Navarro-Ruiz, R. M., Caballero-López, M. J., Del Águila, Á., Muñoz-Galdeano, T., Maza, R. M., & Nieto-Díaz, M. (2017). Diadenosine tetraphosphate (Ap4A) inhibits ATP-induced excitotoxicity: A neuroprotective strategy for traumatic spinal cord injury treatment. *Purinergic Signalling, 13*, 75–87. https://doi.org/10.1007/s11302-016-9541-4.

6. Zheng, H., Zhu, W., Zhao, H., Wang, X., Wang, W., & Li, Z. (2010). Kainic acid-activated microglia mediate increased excitability of rat hippocampal neurons in vitro and in vivo: Crucial role of interleukin-1beta. *Neuroimmunomodulation, 17*, 31–38. https://doi.org/10.1159/000243083.

7. Kuzhandaivel, A., Nistri, A., & Mladinic, M. (2010). Kainate-mediated excitotoxicity induces neuronal death in the rat spinal cord in vitro via a PARP-1 dependent cell death pathway (Parthanatos). *Cellular and Molecular Neurobiology, 30*, 1001–1012. https://doi.org/10.1007/s10571-010-9531-y.

8. Mazzone, L., Margaryan, G., Kuzhandaivel, A., Nasrabady, S. E., Mladinic, M., & Nistri, A. (2010). Kainate-induced delayed onset of excitotoxicity with functional loss unrelated to the extent of neuronal damage in the in vitro spinal cord. *Neuroscience, 168*, 451–462. https://doi.org/10.1016/j.neuroscience.2010.03.055.

9. Mitra, N. K., Goh, T. E. W., Krishnan, T. B., Nadarajah, V. D., Vasavaraj, A. K., & Soga, T. (2013). Effect of intra-cisternal application of kainic acid on the spinal cord and locomotor activity in rats. *International Journal of Clinical and Experimental Pathology, 6*, 1505–1515.

10. Kjell, J., & Olson, L. (2016). Rat models of spinal cord injury: From pathology to potential therapies. *Disease Model Mechanism, 9*, 1125–1137. https://doi.org/10.1242/dmm.025833.

11. Nishida, F., Zanuzzi, C. N., Martínez, A., Barbeito, C. G., & Portiansky, E. L. (2015). Functional and histopathological changes induced by intraparenchymal injection of kainic acid in the rat cervical spinal cord. *Neurotoxicology, 49*, 68–78. https://doi.org/10.1016/j.neuro.2015.05.006.

12. Nishida, F., Sisti, M. S., Zanuzzi, C. N., Barbeito, C. G., & Portiansky, E. L. (2017). Neurons of the rat cervical spinal cord express vimentin and neurofilament after intraparenchymal injection of kainic acid. *Neuroscience Letters, 64*, 103–110. https://doi.org/10.1016/j.neulet.2017.02.029.

13. Zanuzzi, C. N., Nishida, F., Sisti, S., Barbeito, C. G., & Portiansky, E. L. (2019). Reactivity of microglia and astrocytes after an excitotoxic injury induced by kainic acid in the rat spinal cord. *Tissue and Cell, 56*, 31–40. https://doi.org/10.1016/j.tice.2018.11.007.

14. Forostyak, S., Jendelova, P., & Sykova, E. (2013). The role of mesenchymal stromal cells in spinal cord injury, regenerative medicine and possible clinical applications. *Biochimie, 95*, 2257–2270. https://doi.org/10.1016/j.biochi.2013.08.004.

15. Dasari, V. R., Veeravalli, K. K., & Dinh, D. H. (2014). Mesenchymal stem cells in the treatment of spinal cord injuries: A review. *World Journal Stem Cells, 6*(2), 120–133. https://doi.org/10.4252/wjsc.v6.i2.120.

16. Vismara, I., Papa, S., Rossi, F., Forloni, G., & Veglianese, P. (2017). Current options for cell therapy in spinal cord injury. *Trends in Molecular Medicine, 23*, 831–849. https://doi.org/10.1016/j.molmed.2017.07.005.

17. Cofano, F., Boido, M., Monticelli, M., Zenga, F., Ducati, A., Vercelli, A., & Garbossa, D. (2019). Mesenchymal stem cells for spinal cord injury: Current options, limitations, and future of cell therapy. *International Journal Molecular Science, 20*(11), pii: E2698. https://doi.org/10.3390/ijms20112698.

18. Teng, Y. D. (2019). Functional multipotency of stem cells: Biological traits gleaned from neural progeny studies. *Seminars in Cell and Developmental Biology, S1084-9521*(18), 30059–30054. https://doi.org/10.1016/j.semcdb.2019.02.002.

19. Boillée, S., Yamanaka, K., Lobsiger, C. S., Copeland, N. G., Jenkins, N. A., Kassiotis, G., Kollias, G., & Cleveland, D. W. (2006). Onset and progression in inherited ALS determined by motor neurons and microglia. *Science, 312*, 1389–1392. https://doi.org/10.1126/science.1123511.

20. Lee, H. J., Lee, J. K., Lee, H., Carter, J. E., Chang, J. W., Oh, W., Yang, Y. S., Suh, J. G., Lee, B. H., Jin, H. K., & Bae, J. S. (2012). Human umbilical cord blood-derived mesenchymal stem cells improve neuropathology and cognitive impairment in an Alzheimer's disease mouse model through modulation of neuroinflammation. *Neurobiology of Aging, 33*, 588–602. https://doi.org/10.1016/j.neurobiolaging.2010.03.024.

21. Song, C. G., Zhang, Y. Z., Wu, H. N., Cao, X. L., Guo, C. J., Li, Y. Q., Zheng, M. H., & Han, H. (2018). Stem cells: A promising candidate to treat neurological disorders. *Neural Regeneration Research, 13*, 1294–1304. https://doi.org/10.4103/1673-5374.235085.

22. Zappa Villar, M. F., Lehmann, M., Garcia, M. G., Mazzolini, G., Gustavo, R., Morel, G. T., Console, G. M., Podhajcer, O., Reggiani, P. C., & Goya, R. G. (2019). Mesenchymal stem cell therapy improves spatial memory and hippocampal structure in aging rats. *Behavioural Brain Research, 374*, 111887. https://doi.org/10.1016/j.bbr.2019.04.001.

23. Lehmann, M., Zappa-Villar, M. F., García, M. G., Mazzolini, G., Canatelli-Mallat, M., Morel, G. R., Reggiani, P. C., & Goya, R. G.

(2019). Umbilical cord cell therapy improves spatial memory in aging rats. *Stem Cell Reviews, 22*, 612–617. https://doi.org/10.1007/s12015-019-09895-2 [Epub ahead of print].

24. Bayo, J., Fiore, E., Aquino, J. B., Malvicini, M., Rizzo, M., Peixoto, E., Andriani, O., Alaniz, L., Piccioni, F., Bolontrade, M., Podhajcer, O., Garcia, M. G., & Mazzolini, G. (2014). Increased migration of human mesenchymal stromal cells by autocrine motility factor (AMF) resulted in enhanced recruitment towards hepatocellular carcinoma. *PLoS One, 9*(4), e95171. https://doi.org/10.1371/journal.pone.0095171.

25. Dominici, M., Le Blanc, K., Mueller, I., Slaper-Cortenbach, I., Marini, F., Krause, D., Deans, R., Keating, A., Prockop, D., & Horwitz, E. (2006). Minimal criteria for defining multipotent mesenchymal stromal cells. The International Society for Cellular Therapy position statement. *Cytotherapy, 8*, 315–317. https://doi.org/10.1080/14653240600855905.

26. Aquino, J. B., Bolontrade, M. F., García, M. G., Podhajcer, O. L., & Mazzolini, G. (2010). Mesenchymal stem cells as therapeutic tools and gene carriers in liver fibrosis and hepatocellular carcinoma. *Gene Therapy, 17*, 692–708. https://doi.org/10.1038/gt.2010.10.

27. Nishida, F., Zanuzzi, C. N., Márquez, M., Barbeito, C. G., & Portiansky, E. L. (2014). La trepanación vertebral como un método alternativo para la inoculación intraparenquimatosa de diversas suspensiones dentro de la médula espinal. *Analecta Veterinaria, 34*, 11–17.

28. Paxinos, G., & Watson, C. (1998). *The rat brain in stereotaxic coordinates* (4th ed.). Academic: San Diego.

29. Milano, J., Oliveira, S. M., Rossato, M. F., Sauzem, P. D., Machado, P., Beck, P., Zanatta, N., Martins, M. A., Mello, C. F., Rubin, M. A., Ferreira, J., & Bonacorso, H. G. (2008). Antinociceptive effect of novel trihalomethyl-substituted pyrazoline methyl esters in formalin and hot-plate tests in mice. *European Journal of Pharmacology, 581*, 86–96. https://doi.org/10.1016/j.ejphar.2007.11.042.

30. Nishida, F., Morel, G. R., Hereñú, C. B., Schwerdt, J. I., Goya, R. G., & Portiansky, E. L. (2011). Restorative effect of intracerebroventricular Insulin-Like Growth Factor-I gene therapy on motor performance in aging rats. *Neuroscience, 177*, 195–206. https://doi.org/10.1016/j.neuroscience.2011.01.013.

31. Metz, G. A., & Whishaw, I. Q. (2002). Cortical and subcortical lesions impair skilled walking in the ladder rung walking test: A new task to evaluate fore- and hindlimb stepping, placing, and coordination. *Journal of Neuroscience Methods, 115*, 169–179.

32. Portiansky, E. L. (2018). *Análisis Multidimensional de Imágenes Digitales* (2a Ed.). La Plata: Universidad Nacional de La Plata. Formato digital PDF. ISBN:978-950-34-1713-3. http://sedici.unlp.edu.ar/handle/10915/70938

33. Kean, T. J., Lin, P., Caplan, A. L., & Dennis, J. E. (2013). MSCs: Delivery routes and engraftment, cell-targeting strategies, and immune modulation. *Stem Cells International, 2013*, 732742. https://doi.org/10.1155/2013/732742.

34. Huang, P., Freeman, W. D., Edenfield, B. H., Brott, T. G., Meschia, J. F., & Zubair, A. C. (2019). Safety and efficacy of intraventricular delivery of bone marrow-derived mesenchymal stem cells in hemorrhagic stroke model. *Scientific Reports, 9*, 5674. https://doi.org/10.1038/s41598-019-42182-1.

35. Gutova, M., Flores, L., Adhikarla, V., Tsaturyan, L., Tirughana, R., Aramburo, S., Metz, M., Gonzaga, J., Annala, A., Synold, T. W., Portnow, J., Rockne, R. C., & Aboody, K. S. (2019). Quantitative evaluation of intraventricular delivery of therapeutic neural stem cells to orthotopic glioma. *Frontiers in Oncology, 9*, 68. https://doi.org/10.3389/fonc.2019.00068.

36. Chua, S. J., Bielecki, R., Yamanaka, N., Fehlings, M. G., Rogers, I. M., & Casper, R. F. (2010). The effect of umbilical cord blood cells on outcomes after experimental traumatic spinal cord injury. *Spine, 35*, 1520–1526. https://doi.org/10.1097/BRS.0b013e3181c3e963.

37. Kao, C. H., Chen, S. H., Chio, C. C., & Lin, M. T. (2008). Human umbilical cord blood-derived CD34 cells may attenuate spinal cord injury by stimulating vascular endothelial and neurotrophic factors. *Shock, 29*, 49–55. https://doi.org/10.1097/shk.0b013e31805cddce.

38. Ryan, J. M., Barry, F. P., Murphy, J. M., & Mahon, B. P. (2005). Mesenchymal stem cells avoid allogeneic rejection. *Journal of Inflammation (London), 2*, 8. https://doi.org/10.1186/1476-9255-2-8.

39. Gaudet, A. D., & Fonken, L. K. (2018). Glial cells shape pathology and repair after spinal cord injury. *Brain, Behavior, and Immunity, 73*, 133–148. https://doi.org/10.1016/j.bbi.2018.07.012.

40. Lukovic, D., Stojkovic, M., Moreno-Manzano, V., Jendelova, P., Sykova, E., Bhattacharya, S. S., & Erceg, S. (2015). Concise review: Reactive astrocytes and stem cells in spinal cord injury: Good guys or bad guys? *Stem Cells, 33*(4), 1036–1041. https://doi.org/10.1002/stem.

41. Krupa, P., Vackova, I., Ruzicka, J., Zaviskova, K., Dubisova, J., Koci, Z., Turnovcova, K., Urdzikova, L. M., Kubinova, S., Rehak, S., & Jendelova, P. (2018). The effect of human mesenchymal stem cells derived from wharton's jelly in spinal cord injury treatment is dose-dependent and can be facilitated by repeated application. *International Journal of Molecular Sciences, 19*(5), E1503. https://doi.org/10.3390/ijms19051503.

42. Chen, C., Chen, F., Yao, C., Shu, S., Feng, J., Hu, X., Hai, Q., Yao, S., & Chen, X. (2016). Intrathecal injection of human umbilical cord-derived mesenchymal stem cells ameliorates neuropathic pain in rat. *Neurochemical Research, 41*, 3250–3260. https://doi.org/10.1007/s11064-016-2051-5.

43. Salgado, A. J., Fraga, J. S., Mesquita, A. R., Neves, N. M., Reis, R. L., & Sousa, N. (2010). Role of human umbilical cord mesenchymal progenitors conditioned media in neuronal/glial cell densities, viability, and proliferation. *Stem Cells and Development, 19*, 1067–1074. https://doi.org/10.1089/scd.2009.0279.

44. Abbaszadeh, H. A., Tiraihi, T., Noori-Zadeh, A., Delshad, A. R., Sadeghizade, M., & Taheri, T. (2015). Human ciliary neurotrophic factor-overexpressing stable bone marrow stromal cells in the treatment of a rat model of traumatic spinal cord injury. *Cytotherapy, 17*, 912–921. https://doi.org/10.1016/j.jcyt.2015.03.689.

45. Hofstetter, C. P., Schwarz, E. J., Hess, D., Widenfalk, J., El Manira, A., Prockop, D. J., & Olson, L. (2002). Marrow stromal cells form guiding strands in the injured spinal cord and promote recovery. *Proceedings of the National Academy of Sciences of the United States of America, 99*, 2199–2204. https://doi.org/10.1073/pnas.042678299.

46. Ohta, M., Suzuki, Y., Noda, T., Ejiri, Y., Dezawa, M., Kataoka, K., Chou, H., Ishikawa, N., Matsumoto, N., Iwashita, Y., Mizuta, E., Kuno, S., & Ide, C. (2004). Bone marrow stromal cells infused into the cerebrospinal fluid promote functional recovery of the injured rat spinal cord with reduced cavity formation. *Experimental Neurology, 187*, 266–278. https://doi.org/10.1016/j.expneurol.2004.01.021.

47. Falkner, S., Grade, S., Dimou, L., Conzelmann, K. K., Bonhoeffer, T., Götz, M., Hübener, M., Wuttke, T. V., Markopoulos, F., Padmanabhan, H., & Wheeler, A. P. (2016). Transplanted embryonic neurons integrate into adult neocortical circuits. *Nature, 539*, 248–253. https://doi.org/10.1038/nature20113.

48. Wuttke, T. V., Markopoulos, F., Padmanabhan, H., Wheeler, A. P., Murthy, V. N., & Macklis, J. D. (2018). Developmentally primed cortical neurons maintain fidelity of differentiation and establish appropriate functional connectivity after transplantation. *Nature Neuroscience, 21*, 517–529. https://doi.org/10.1038/s41593-018-0098-0.

49. Abrams, M. B., Dominguez, C., Pernold, K., Reger, R., Wiesenfeld-Hallin, Z., Olson, L., & Prockop, D. (2009). Multipotent mesenchymal stromal cells attenuate chronic inflammation and injury-induced sensitivity to mechanical stimuli in

experimental spinal cord injury. *Restorative Neurology and Neuroscience, 27*, 307–321. https://doi.org/10.3233/RNN-2009-0480.

50. Kang, S. K., Shin, M. J., Jung, J. S., Kim, Y. G., & Kim, C. H. (2006). Autologous adipose tissue-derived stromal cells for treatment of spinal cord injury. *Stem Cells and Development, 15*, 583–594. https://doi.org/10.1089/scd.2006.15.583.

51. Lin, W., Xu, L., Zwingenberger, S., Gibon, E., Goodman, S. B., & Li, G. (2017). Mesenchymal stem cells homing to improve bone healing. *Journal of Orthopaedic Translation, 9*, 19–27. https://doi.org/10.1016/j.jot.2017.03.002.

52. Drommelschmidt, K., Serdar, M., Bendix, I., Herz, J., Bertling, F., Prager, S., Keller, M., Ludwig, A.-K., Duhan, V., Radtke, S., de Miroschedji, K., Horn, P. A., van de Looji, Y., Giebel, B., & Felderhoff-Müser, U. (2017). Mesenchymal stem cell-derived extracellular vesicles ameliorate inflammation-induced preterm brain injury. *Brain, Behavior and Immunity, 60*, 220–232. https://doi.org/10.1016/j.bbi.2016.11.011.

53. Kwon, M. S., Noh, M. Y., Oh, K. W., Cho, K. A., Kang, B. Y., Kim, K. S., Kim, Y. S., & Kim, S. H. (2014). The immunomodulatory effects of human mesenchymal stem cells on peripheral blood mononuclear cells in ALS patients. *The Journal of Neurochemistry, 131*, 206–218. https://doi.org/10.1111/jnc.12814.

54. Sheikh, A. M., Nagai, A., Wakabayashi, K., Narantuya, D., Kobayashi, S., Yamaguchi, S., & Kim, S. U. (2011). Mesenchymal stem cell transplantation modulates neuroinflammation in focal cerebral ischemia: Contribution of fractalkine and IL-5. *Neurobiology of Disease, 41*, 717–724. https://doi.org/10.1016/j.nbd.2010.12.009.

55. Yan, K., Zhang, R., Sun, C., Chen, L., Li, P., Liu, Y., Peng, L., Sun, H., Qin, K., Chen, F., Lv, B., Du, M., Zou, Y., Cai, Y., Qin, L., Tang, Y., & Jiang, X. (2013). Bone marrow-derived mesenchymal stem cells maintain the resting phenotype of microglia and inhibit microglial activation. *PLoS One, 8*, e84116. https://doi.org/10.1371/journal.pone.0084116.

56. Wang, L., Pei, S., Han, L., Guo, B., Li, Y., Duan, R., Yao, Y., Xue, B., Chen, X., & Jia, Y. (2018). Mesenchymal stem cell-derived exosomes reduce A1 astrocytes via downregulation of phosphorylated NFκB P65 subunit in spinal cord injury. *Cellular Physiology and Biochemistry, 50*(4), 1535–1559. https://doi.org/10.1159/000494652.

57. Kim, C., Kim, H. J., Lee, H., Lee, H., Lee, S. J., Lee, S. T., Yang, S. R., & Chung, C. K. (2019). Mesenchymal stem cell transplantation promotes functional recovery through MMP2/STAT3 related astrogliosis after spinal cord injury. *International Journal of Stem Cells, 12*(2), 331–339. https://doi.org/10.15283/ijsc18133.

58. Zamanian, J. L., Xu, L., Foo, L. C., Nouri, N., Zhou, L., Giffard, R. G., & Barres, B. A. (2012). Genomic analysis of reactive astrogliosis. *Journal of Neuroscience, 32*, 6391–6410. https://doi.org/10.1523/JNEUROSCI.6221-11.2012.

59. Liddelow, S. A., Guttenplan, K. A., Clarke, L. E., Bennett, F. C., Bohlen, C. J., Schirmer, L., Bennett, M. L., Münch, A. E., Chung, W. S., Peterson, T. C., Wilton, D. K., Frouin, A., Napier, B. A., Panicker, N., Kumar, M., Buckwalter, M. S., Rowitch, D. H., Dawson, V. L., Dawson, T. M., Stevens, B., & Barres, B. A. (2017). Neurotoxic reactive astrocytes are induced by activated microglia. *Nature, 541*(7638), 481–487. https://doi.org/10.1038/nature21029.

60. Liu, W., Wang, Y., Gong, F., Rong, Y., Luo, Y., Tang, P., Zhou, Z., Zhou, Z., Xu, T., Jiang, T., Yang, S., Yin, G., Chen, J., Fan, J., & Cai, W. (2019). Exosomes derived from bone mesenchymal stem cells repair traumatic spinal cord injury by suppressing the activation of a1 neurotoxic reactive astrocytes. *Journal of Neurotrauma, 36*(3), 469–484. https://doi.org/10.1089/neu.2018.5835.

61. Zappa Villar, M. F., López Hanotte, J., Pardo, J., Morel, G. R., Mazzolini, G., García, M. G., & Reggiani, P. C. (2019). Mesenchymal stem cells therapy improved the streptozotocin-induced behavioral and hippocampal impairment in rats. *Molecular Neurobiology*, 1–16. https://doi.org/10.1007/s12035-019-01729-z [Epub ahead of print].

62. Wilhelmsson, U., Faiz, M., de Pablo, Y., Sjöqvist, M., Andersson, D., Widestrand, A., Potokar, M., Stenovec, M., Smith, P. L., Shinjyo, N., Pekny, T., Zorec, R., Ståhlberg, A., Pekna, M., Sahlgren, C., & Pekny, M. (2012). Astrocytes negatively regulate neurogenesis through the Jagged 1-mediated Notch pathway. *Stem Cells, 30*, 2320–2329. https://doi.org/10.1002/stem.1196.

63. Shi, W., Huang, C. J., Xu, X. D., Jin, G. H., Huang, R. Q., Huang, J. F., Chen, Y. N., Ju, S. Q., Wang, Y., Shi, Y. W., Qin, J. B., Zhang, Y. Q., Liu, Q. Q., Wang, X. B., Zhang, X. H., & Chen, J. (2016). Transplantation of RADA16-BDNF peptide scaffold with human umbilical cord mesenchymal stem cells forced with CXCR4 and activated astrocytes for repair of traumatic brain injury. *Acta Biomaterialia, 45*, 247–261. https://doi.org/10.1016/j.actbio.2016.09.001.

64. Huang, J. H., Yin, X. M., Xu, Y., Xu, C. C., Lin, X., Ye, F. B., Cao, Y., & Lin, F. Y. (2017). Systemic administration of exosomes released from mesenchymal stromal cells attenuates apoptosis, inflammation, and promotes angiogenesis after spinal cord injury in rats. *Journal of Neurotrauma, 34*(24), 3388–3396. https://doi.org/10.1089/neu.2017.5063.

65. Wrathall, J. R., Teng, Y. D., & Marriott, R. (1997). Delayed antagonism of AMPA/kainate receptors reduces long-term functional deficits resulting from spinal cord trauma. *Experimental Neurology, 145*(2 Pt 1), 565–573.